Article

Conformational Dependence of Hemoglobin Reactivity under High Viscosity Conditions: The Role of Solvent Slaved Dynamics

Uri Samuni, Camille J. Roche, David Dantsker, and Joel M. Friedman

J. Am. Chem. Soc., **2007**, 129 (42), 12756-12764• DOI: 10.1021/ja072342b • Publication Date (Web): 02 October 2007

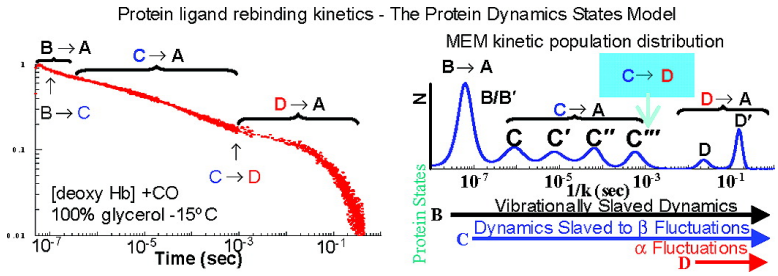

More About This Article

Additional resources and features associated with this article are available within the HTML version:

- Supporting Information
- Links to the 1 articles that cite this article, as of the time of this article download
- Access to high resolution figures
- Links to articles and content related to this article
- Copyright permission to reproduce figures and/or text from this article

View the Full Text HTML

J|A|C|S
ARTICLES
Published on Web 10/02/2007

Conformational Dependence of Hemoglobin Reactivity under High Viscosity Conditions: The Role of Solvent Slaved Dynamics

Uri Samuni, Camille J. Roche, David Dantsker, and Joel M. Friedman*

Contribution from the Department of Physiology and Biophysics, Albert Einstein College of Medicine, Bronx, New York 10461

Received April 3, 2007; E-mail: jfriedma@aecom.yu.edu

Abstract: The concept of protein dynamic states is introduced. This concept is based on (i) protein dynamics being organized hierarchically with respect to solvent slaving and (ii) which tier of dynamics is operative over the time window of a given measurement. The protein dynamic state concept is used to analyze the kinetic phases derived from the recombination of carbon monoxide to sol−gel-encapsulated human adult hemoglobin (HbA) and select recombinant mutants. The temperature-dependent measurements are made under very high viscosity conditions obtained by bathing the samples in an excess of glycerol. The results are consistent with a given tier of solvent slaved dynamics becoming operative at a time delay (with respect to the onset of the measurement) that is primarily solvent- and temperature-dependent. However, the functional consequences of the dynamics are protein- and conformation-specific. The kinetic traces from both equilibrium populations and trapped allosteric intermediates show a consistent progression that exposes the role of both conformation and hydration in the control of reactivity. Iron−zinc symmetric hybrid forms of HbA are used to show the dramatic difference between the kinetic patterns for T state α and β subunits. The overall results support a model for allostery in HbA in which the ligand-binding-induced transition from the deoxy T state to the high -affinity R state proceeds through a progression of T state intermediates.

Introduction

The relationship between protein dynamics and protein function is an integral aspect of the ongoing pursuit of a detailed mechanistic picture of how proteins work. Studies that address the structural contributions to protein function are relatively straightforward. There are agreed-upon protocols for both generating and analyzing structural data. In contrast, studies addressing the functional role of dynamics are problematic on many levels. There is the experimental challenge of how to couple measurements of function with those that probe dynamics. On a very fundamental level, there is also the issue of how to organize the complex array of protein dynamics into groupings that are useful or appropriate for exposing functional consequences. In the present treatment, we build upon several recent advances to develop a strategy to address these challenges with respect to analyzing how dynamics contribute to the conformational dependence of ligand recombination in human adult hemoglobin (HbA).

The evolving concept of solvent slaving[1−4] is used as an organizing principle that provides a framework for defining and characterizing categories of protein dynamics on the basis of the degree to which they are coupled, i.e., "slaved", to specific molecular motions within the surrounding solvent. This approach gives rise to a hierarchy of dynamics that also implies a hierarchy of time scales over which the specific tier of dynamics is or is not operative with respect to some observed functional process. This type of organizational structure has many benefits, in that it facilitates (i) comparing different solvents with respect to influence on the dynamics and functional properties of a given protein, (ii) comparing effects of a specific solvent on the dynamics and functional properties of different proteins, and (iii) exposing correlations between temporal sequences of changes in functional properties and temporal sequences for the onset of the influence of the different solvent-dependent dynamics.

Exploiting the inherent temporal hierarchy associated with the solvent slaving-based hierarchy of dynamics in an experimental modality is problematic. Ideally, one requires a functional process that (i) can be triggered on a time scale that is fast compared to the onset of the influence of the different tiers of dynamics and (ii) persists long enough to be influenced by the temporal progression of dynamics-driven processes. Ligand recombination subsequent to photodissociation in heme proteins is an ideal process for testing and probing these concepts. The duration of the kinetic process can easily be tuned over a very wide range of time scales (picoseconds to seconds) on the basis of choice of protein, ligand, conformation, and mutational/chemical modifications. The kinetic traces for ligand recombination display a temperature- and solvent-dependent progression

(1) Fenimore, P. W.; Frauenfelder, H.; McMahon, B. H.; Parak, F. G. *Proc. Natl. Acad. Sci. U.S.A.* **2002**, *99*, 16047−16051.
(2) Lubchenko, V.; Wolynes, P. G.; Frauenfelder, H. *J. Phys. Chem. B Condens. Matter Mater. Surf. Interfaces Biophys.* **2005**, *109*, 7488−7499.
(3) Frauenfelder, H.; Fenimore, P. W.; Chen, G.; McMahon, B. H. *Proc. Natl. Acad. Sci. U.S.A.* **2006**, *103*, 15469−15472.
(4) Frauenfelder, H.; Fenimore, P. W.; McMahon, B. H. *Biophys. Chem.* **2002**, *98*, 35−48.

10.1021/ja072342b CCC: $37.00

of phases. Typically, as one increases the temperature starting at very low cryogenic temperatures, one observes the appearance of new slower phases that originate from the activation of dynamics-mediated processes that cause the slowing. The temperature dependence of the transition points where the initially observed phase ends and a new slower phase starts is thus directly related to the temperature-dependent onset of the influence of the tier of dynamics that is now being thermally activated.

The recombination of CO to photodissociated COMb has been the prototype process for studies relating reactivity to dynamics.[5−9] CO recombination studies on myoglobin (Mb) at cryogenic temperatures have resulted in many new concepts that now have widespread significance and application. These concepts include rough energy landscape, inverse temperature effect, hierarchical organization for both structure and dynamics, and solvent slaving. Similarly, the spectroscopic changes initiated by and occurring subsequent to photodissociation of COMb have exposed many new phenomena, such as kinetic hole burning,[10−17] remote ligand docking sites,[18,19] and conformational relaxation,[20−23] that directly link dynamics with reactivity. Many of these concepts have been further expanded through the combined tuning of temperature and viscosity as a means of modulating dynamics.[24−28]

The use of sol−gel encapsulation of proteins has proven to be an additional tool for isolating the functional consequences of relaxation processes and equilibrium fluctuations. Studies show that sol−gel encapsulation of Mb[29,30] and Hb[31−35] can greatly slow conformational changes initiated by ligand binding or release. As a consequence, an initial global tertiary/quaternary structure can, in effect, be "locked in" for time scales that often greatly exceed the time scale for measuring functional processes. This approach provides a direct method for comparing ligand rebinding kinetics in equilibrium and nonequilibrium populations of both Mb[29] and HbA.[34,36,37] Additionally, sol−gel matrices allow facile exchange of solvents, thus providing a convenient method of bathing both equilibrium and nonequilibrium populations in high-viscosity solvents.[26−28,34,38−41] This approach has proven very effective in enhancing features in the recombination traces that are signatures of specific dynamics-mediated transitions or events. For example, the CO recombination kinetics from sol−gel-encapsulated COHbA bathed in glycerol-containing buffer display features indicative of remote docking sites similar to the Xe cavities observed in Mb.[42] In the case of sol−gel-encapsulated Mb's, replacing the bathing buffer with an excess of pure glycerol results in temperature-dependent kinetic traces at ambient temperatures that manifest many of the features seen at cryogenic temperatures.[26,27]

The results from the Mb studies utilizing both glycerol-bathed sol−gels and trehalose glass matrices have led us to a new framework for relating dynamics to functionality that introduces a new nomenclature and model for the protein states based on which tiers of dynamics are active during the measurement.[43] This new model, referred to as the protein dynamic state model, and the associated nomenclature avoid the ambiguity of basing the assignment of kinetic phases on either location of the dissociated ligand or specific relaxation events. Instead, it is based on which tier of dynamics is operative during the observation window. Since the different tiers of dynamics become operational on time scales based on the solvent dynamics to which they are or are not slaved, the transition between these protein-dynamics-based states is overwhelmingly determined by the particular temperature and solvent. In contrast, the functional consequences of the onset of the influence of specific tiers of dynamics are expected to be protein-specific.

The basic idea is that, from the instant of photodissociation, there is a temporal progression for the onset of the influence,

(5) Austin, R. H.; Beeson, K.; Eisenstein, L.; Frauenfelder, H.; Gunsalus, I. C.; Marshall, V. P. *Science* **1973**, *181*, 541−543.
(6) Austin, R. H.; Beeson, K. W.; Eisenstein, L.; Frauenfelder, H.; Gunsalus, I. C. *Biochemistry* **1975**, *14*, 5355−5373.
(7) Frauenfelder, H.; Sligar, S. G.; Wolynes, P. G. *Science* **1991**, *254*, 1598−1603.
(8) Frauenfelder, H. *Nat. Struct. Biol.* **1995**, *2*, 821−823.
(9) Frauenfelder, H.; McMahon, B. H.; Fenimore, P. W. *Proc. Natl. Acad. Sci. U.S.A.* **2003**, *100*, 8615−8617.
(10) Berendzen, J.; Braunstein, D. *Proc. Natl. Acad. Sci. U.S.A.* **1990**, *87*, 1−5.
(11) Campbell, B. F.; Chance, M. R.; Friedman, J. M. *Science* **1987**, *238*, 373−376.
(12) Huang, J.; Ridsdale, A.; Wang, J.; Friedman, J. M. *Biochemistry* **1997**, *36*, 14353−14365.
(13) Nienhaus, G. U.; Mourant, J. R.; Frauenfelder, H. *Proc. Natl. Acad. Sci. U.S.A.* **1992**, *89*, 2902−2906.
(14) Srajer, V.; Champion, P. M. *Biochemistry* **1991**, *30*, 7390−7402.
(15) Chavez, M. D.; Courtney, S. H.; Chance, M. R.; Kiula, D.; Nocek, J.; Hoffman, B. M.; Friedman, J. M.; Ondrias, M. R. *Biochemistry* **1990**, *29*, 4844−4852.
(16) Levantino, M.; Cupane, A.; Zimanyi, L. *Biochemistry* **2003**, *42*, 4499−4505.
(17) Agmon, N. *Biochemistry* **1988**, *27*, 3507−3511.
(18) Kriegl, J. M.; Nienhaus, K.; Deng, P.; Fuchs, J.; Nienhaus, G. U. *Proc. Natl. Acad. Sci. U.S.A.* **2003**, *100*, 7069−7074.
(19) Lamb, D. C.; Nienhaus, K.; Arcovito, A.; Draghi, F.; Miele, A. E.; Brunori, M.; Nienhaus, G. U. *J. Biol. Chem.* **2002**, *277*, 11636−11644.
(20) Abadan, Y.; Chien, E. Y.; Chu, K.; Eng, C. D.; Nienhaus, G. U.; Sligar, S. G. *Biophys. J.* **1995**, *68*, 2497−2504.
(21) Ahmed, A. M.; Campbell, B. F.; Caruso, D.; Chance, M. R.; Chavez, M. D.; Courtney, S. H.; Friedman, J. M.; Iben, I. E. T.; Ondrias, M. R.; Yang, M. *Chem. Phys.* **1991**, *158*, 329−351.
(22) Ansari, A.; Berendzen, J.; Bowne, S. F.; Frauenfelder, H.; Iben, I. E.; Sauke, T. B.; Shyamsunder, E.; Young, R. D. *Proc. Natl. Acad. Sci. U.S.A.* **1985**, *82*, 5000−5004.
(23) Ansari, A.; Berendzen, J.; Braunstein, D.; Cowen, B. R.; Frauenfelder, H.; Hong, M. K.; Iben, I. E.; Johnson, J. B.; Ormos, P.; Sauke, T. B.; Scholl, R.; Schulte, A.; Steinbach, P. J.; Vittitow, J.; Young, R. D. *Biophys. Chem.* **1987**, *26*, 337−355.
(24) Hagen, S. J.; Hofrichter, J.; Eaton, W. A. *J. Phys. Chem.* **1996**, *100*, 12008−12021.
(25) Ansari, A.; Jones, C. M.; Henry, E. R.; Hofrichter, J.; Eaton, W. A. *Science* **1992**, *256*, 1796−1798.
(26) Dantsker, D.; Roche, C.; Samuni, U.; Blouin, G.; Olson, J. S.; Friedman, J. M. *J. Biol. Chem.* **2005**, *280*, 38740−38755.
(27) Dantsker, D.; Samuni, U.; Friedman, J. M.; Agmon, N. *Biochim. Biophys. Acta* **2005**, *1749*, 234−251.
(28) Dantsker, D.; Samuni, U.; Ouellet, Y.; Wittenberg, B. A.; Wittenberg, J. B.; Milani, M.; Bolognesi, M.; Guertin, M.; Friedman, J. M. *J. Biol. Chem.* **2004**, *279*, 38844−38853.
(29) Samuni, U.; Dantsker, D.; Khan, I.; Friedman, A. J.; Peterson, E.; Friedman, J. M. *J. Biol. Chem.* **2002**, *277*, 25783−25790.
(30) Shibayama, N.; Saigo, S. *J. Am. Chem. Soc.* **2003**, *125*, 3780−3783.
(31) Abbruzzetti, S.; Viappiani, C.; Bruno, S.; Bettati, S.; Bonaccio, M.; Mozzarelli, A. *J. Nanosci. Nanotechnol.* **2001**, *1*, 407−415.
(32) Bettati, S.; Mozarrelli, A. *J. Biol. Chem.* **1997**, *272*, 32050−32055.
(33) Das, T. K.; Khan, I.; Rousseau, D. L.; Friedman, J. M. *Biospectroscopy* **1999**, *5*, 64−70.
(34) Khan, I.; Shannon, C. F.; Dantsker, D.; Friedman, A. J.; Perez-Gonzalez-de Apodaca, J.; Friedman, J. M. *Biochemistry* **2000**, *39*, 16099−16109.
(35) Shibayama, N.; Saigo, S. *J. Mol. Biol.* **1995**, *25*, 203−209.
(36) Abbruzetti, S.; Viappiani, C.; Bruno, S.; Mozzarelli, A. *Chem. Phys. Lett.* **2001**, *346*, 430−436.
(37) Samuni, U.; Dantsker, D.; Juszczak, L. J.; Bettati, S.; Ronda, L.; Mozzarelli, A.; Friedman, J. M. *Biochemistry* **2004**, *43*, 13674−13682.
(38) Dantsker, D.; Samuni, U.; Friedman, A. J.; Yang, M.; Ray, A.; Friedman, J. M. *J. Mol. Biol.* **2002**, *315*, 239−251.
(39) Sottini, S.; Abbruzzetti, S.; Viappiani, C.; Bettati, S.; Ronda, L.; Mozzarelli, A. *J. Phys. Chem. B Condens. Matter Mater. Surf. Interfaces Biophys.* **2005**, *109*, 11411−11413.
(40) Sottini, S.; Abbruzzetti, S.; Viappiani, C.; Ronda, L.; Mozzarelli, A. *J. Phys. Chem. B Condens. Matter Mater. Surf. Interfaces Biophys.* **2005**, *109*, 19523−19528.
(41) Sottini, S.; Viappiani, C.; Ronda, L.; Bettati, S.; Mozzarelli, A. *J. Phys. Chem. B Condens. Matter Mater. Surf. Interfaces Biophys.* **2004**, *108*, 8475−8484.
(42) Sottini, S.; Abbruzzetti, S.; Spyrakis, F.; Bettati, S.; Ronda, L.; Mozzarelli, A.; Viappiani, C. *J. Am. Chem. Soc.* **2005**, *127*, 17427−17432.
(43) Samuni, U.; Dantsker, D.; Roche, C. J.; Friedman, J. M. *Gene* **2007**, *398*, 234−248.

i.e., activation, of different tiers of dynamics. The tiers are organized hierarchically on the basis of the degree of solvent slaving. In the current analysis, we define three major tiers of dynamics: the B, C, and D state tiers. The B state refers to the state of the protein that exists during the temporal window when only internal-vibrations-driven dynamics are operational, such as occur at very low cryogenic conditions or for very short intervals following photolysis at higher temperatures. The C state refers to the state of the protein that exists when the protein is experiencing the influence of those dynamics that are slaved to the localized low-amplitude solvent motions (e.g., librations) typically associated with β fluctuations of the hydration shell waters.[1−4] The D state refers to the state of the protein that is observed when the protein is under the influence of those dynamics that are slaved to the large-amplitude motions of the bulk solvent (e.g., those connected with dielectric relaxation), such as those known as α fluctuations.[1−4] The ordering based on the degree of solvent slaving and the associated activation energies for the α and β slaved dynamics gives rise to the temporal progression. Over a given observational time window starting at a given time point, the protein will sequentially reflect behavior indicative of a progression from the B to C to D state.

In our earlier work on Mb and Mb mutants,[26,27] it was shown that:

1. During the lifetime of the B state, the dissociated ligand is typically confined to the distal heme pocket.

2. The C state tier of dynamics includes small-amplitude side-chain fluctuations and relaxations that can both facilitate ligand diffusion between accessible volumes within the protein matrix (e.g., distal heme pocket and Xe cavities) and increase the barrier for recombination.

3. The D state tier of dynamics contains the large volume changing fluctuations that permit both the entering and exiting of ligands and water into and out of the protein and the opening of internal channels closed by the presence of aromatic side chains (e.g., the E11(68)W side chain blocking access between the distal heme pocket (DHP) and the adjacent Xe4 cavity in Mb). Vitrification of the bulk solvent, as in the case of a trehalose glass, results in the damping of these large protein motions which require substantial translation of the bulk solvent.

In the present study, the validity and applicability of the new framework[43] is explored for different tertiary/quaternary conformations of sol−gel-encapsulated Hb's bathed in an excess of pure glycerol. Additionally, a novel tool is introduced for analysis of the kinetics based on the detection and comparison of the time points corresponding to the transition between dynamic states. The premise behind this approach is that a given recombination process (e.g., C→A) terminates at the point when a new tier of dynamics becomes activated/operational. Under the influence of this new tier of dynamics (e.g., D), the new recombination process (e.g., D→A *vis-à-vis* the faster C→A) will be noticeably slower than the preceding recombination phase due to any of a number of new dynamics-mediated relaxation processes that raise the enthalpic and entropic barriers for recombination. The typical experimental manifestation of the onset of the new tier of dynamics is the production of a "break" in the kinetic trace that cuts off the existing process and leads to a new, clearly distinct slower phase that is discernible in the maximum entropy method (MEM) population analysis as well as in the trace itself. (For details on the procedure for determination of the dynamic states' transition points, see the Supporting Information.) HbA provides a rich assortment of conformations that can be trapped within the sol−gel matrix. Using previously established protocols,[29,34] we are able to generate the high-viscosity recombination kinetics for both R state and low- and high-affinity T state forms of HbA. Starting with a sol−gel-encapsulated deoxyHbA sample, the initial species formed immediately after CO is added are designated low-affinity T (LT), since they retain a low affinity distribution and can be further trapped by replacing the buffer with 100% glycerol. The LT samples can be allowed to evolve for a time duration that can vary between hours to weeks, depending on the gelation protocol, until spectroscopic signatures of high-affinity T (HT) are observed.[37,44] The high-viscosity kinetic patterns from sol−gel-stabilized allosteric intermediates such as the low-affinity and high-affinity liganded T state species[37,44,45] are shown to also be obtainable from stable equilibrium populations of mutant forms of HbA. To that end, we used the Hb(βW37E) mutant that has been shown to undergo the LT-to-HT state conformational change upon ligand binding,[44,46−49] as well as double and triple mutant (HbD and HbT) modifications of HbPresbyterian(βN108K),[50−55] i.e., HbαV96W/βN108K[51]and HbαL29F/ αV96W/βN108K,[56,57] which are very low affinity hemoglobins that display T state NMR signatures even for the fully liganded derivatives.[56,57] Large α/β subunit differences in the high-viscosity kinetic patterns from half-liganded T state forms of HbA are exposed using encapsulated FeCO/Zn hybrid derivatives.[58−62] The new protein dynamics-based model provides a coherent framework to explore the origin of variations in kinetic patterns as a function of solvent, conformation, and specific subunit.

Methods

All methods used in this work are described in previous publications as well as in the Supporting Information. Sol−gel-encapsulated samples were made using our well-established protocol that is especially

(44) Samuni, U.; Roche, C. J.; Dantsker, D.; Juszczak, L. J.; Friedman, J. M. *Biochemistry* **2006**, *45*, 2820−2835.
(45) Bruno, S.; Bonaccio, M.; Bettati, S.; Rivetti, C.; Viappiani, C.; Abbruzzetti, S.; Mozzarelli, A. *Protein Sci.* **2001**, *10*, 2401−2407.
(46) Peterson, E. S.; Friedman, J. M. *Biochemistry* **1998**, *37*, 4346−4357.
(47) Kavanaugh, J. S.; Weydert, J. A.; Rogers, P. H.; Arnone, A. *Biochemistry* **1998**, *37*, 4358−4373.
(48) Kwiatkowski, L. D.; Hui, H. L.; Wierzba, A.; Noble, R. W.; Walder, R. Y.; Peterson, E. S.; Sligar, S. G.; Sanders, K. E. *Biochemistry* **1998**, *37*, 4325−4335.
(49) Kavanaugh, J. S.; Rogers, P. H.; Arnone, A. *Biochemistry* **2005**, *44*, 6101−6121.
(50) Manjula, B. N.; Malavalli, A.; Prabhakaran, M.; Friedman, J. M.; Acharya, A. S. *Protein Eng.* **2001**, *14*, 359−366.
(51) Tsai, C. H.; Shen, T. J.; Ho, N. T.; Ho, C. *Biochemistry* **1999**, *38*, 8751−8761.
(52) O'Donnell, J. K.; Birch, P.; Parsons, C. T.; White, S. P.; Okabe, J.; Martin, M. J.; Adams, C.; Sundarapandiyan, K.; Manjula, B. N.; Acharya, A. S. *J. Biol. Chem.* **1994**, *269*, 27692−27699.
(53) Moo-Penn, W. F.; Wolff, J. A.; Simon, G.; Vacek, M.; Jue, D. L.; Johnson, M. H. *FEBS Lett.* **1978**, *92*, 53−56.
(54) Acharya, S. A.; Malavalli, A.; Peterson, E.; Sun, P. D.; Ho, C.; Prabhakaran, M.; Arnone, A.; Manjula, B. N.; Friedman, J. M. *J. Protein Chem.* **2003**, *22*, 221−230.
(55) Gottfried, D. S.; Manjula, B. N.; Malavalli, A.; Acharya, A. S.; Friedman, J. M. *Biochemistry* **1999**, *38*, 11307−11315.
(56) Jeong, S. T.; Ho, N. T.; Hendrich, M. P.; Ho, C. *Biochemistry* **1999**, *38*, 13433−13442.
(57) Tsai, C. H.; Ho, C. *Biophys. Chem.* **2002**, *98*, 15−25.
(58) Fiechtner, M. D.; McLendon, G.; Bailey, M. W. *Biochem. Biophys. Res. Commun.* **1980**, *96*, 618−625.
(59) Huang, Y.; Doyle, M. L.; Ackers, G. K. *Biophys. J.* **1996**, *71*, 2094−2105.
(60) Hui, H. L.; Kwiatkowski, L. D.; Karasik, E.; Colby, J. E.; Noble, R. W. *Biochemistry* **2004**, *43*, 7843−7850.
(61) Miyazaki, G.; Morimoto, H.; Yun, K. M.; Park, S. Y.; Nakagawa, A.; Minagawa, H.; Shibayama, N. *J. Mol. Biol.* **1999**, *292*, 1121−1136.

effective in slowing conformational relaxations.[29,34,44] Samples of Hb in trehalose-derived glassy matrices were prepared as previously described.[26,38,63] Kinetics of CO rebinding to HbA were generated and displayed on log−log plots as described previously.[5,6,29,38] The maximum entropy method was used to extract kinetically distinct populations from the kinetic data.[26,39,44,64−68] Full details of the materials and experimental techniques, including the method for identifying the transition points on the kinetic traces, are contained in the Supporting Information.

Results and Discussion

Three Kinetic Phases Defined on the Basis of the Influence of Solvent Slaved Dynamics. Figure 1 shows a representative CO recombination trace from a glycerol-bathed sol−gel-encapsulated HbA sample. The overall recombination trace from the liganded T state at −15 °C is divided into three phases on the basis of the earlier work on Mb.[26,27,43] The kinetic phases are delineated and analyzed using the protein dynamic state model[43] that was successfully used to describe the relationship between tiers of dynamics and the kinetic phases observed for Mb.[43]

The B→A, C→A, and D→A transitions shown in Figure 1 refer to the CO recombination phases that occur under the influence of the B, C, and D state tiers of dynamics, respectively, with A being the corresponding state in which the ligand is covalently bound to the heme iron. These three phases were observed and characterized in a large series of Mb mutants.[26,27] The similarity between the kinetic patterns seen for Mb and HbA implies that similar processes occur for both proteins. As a consequence, we utilize the Mb results as a basis for description of the phases seen in HbA.

The B→A phase is a geminate phase, also named Process I in earlier cryogenic literature. Two B state phases have been identified in Mb, the B→A phase and the slower B′→A phase. The latter is attributed to recombination of CO that has accessed more remote sites within the DHP. For low-affinity species such as the T state Hb sample whose kinetics are shown in Figure 1, the two B state recombination phases are often merged, and consequently we label the B state MEM population with a B/B′ designation. The C→A phase is also a geminate phase, but the influence of the activated C state tier of side-chain fluctuations usually results in the dissociated ligand accessing all of the accessible cavities over the lifetime of the C state. As a consequence, the C→A recombination can be both entropically slowed due to the enhanced accessible volume and modulated by introducing Xe gas to decrease the volume associated with the Xe cavities. Additionally, there is a progression of relaxations that occur within the C state (e.g., C→C′, C′→C″) that cause the appearance of a progression of slower C′→A, C″→A recombination phases, as revealed in the MEM distributions, that can be attributed to side-chain relaxations of distal heme pocket residues.[26,27] The D state recombination occurs during the time window where ligands and water molecules from the solvent can access the DHP and internal ligands can escape into the solvent. It should be noted that, in the D state, under conditions where the CO concentration is not rate-limiting, a D→A recombination is essentially indistinguishable from the bimolecular or solvent recombination phases. The three families of kinetic phases are temporally separated from each other by transitions between the different dynamic states (e.g., B→C, C→D) as shown in Figure 1. These transitions are manifested in the kinetic traces as breaks (i.e., a large, visibly discernible decrease in the slope of a recombination phase) that herald the onset of new slower phases (see Supporting Information for a description of how these breaks can be analytically determined). No such break in a recombination trace is observed under conditions where the dynamics responsible for the onset of the next phase are not activated (vide infra).

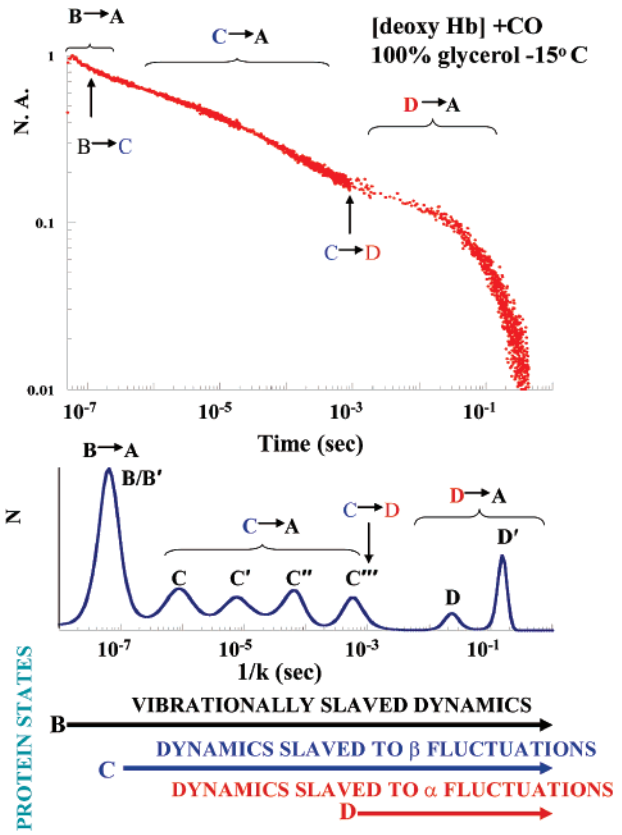

Figure 1. (i) Log−log CO recombination trace (normalized absorbance, NA, versus time subsequent to excitation) at −15 °C for the low-affinity T state form of HbA encapsulated in a porous sol−gel ([deoxyHbA]+CO), bathed in an excess of pure glycerol (top). (ii) Maximum entropy method-derived kinetic populations displayed as normalized population (*N*) versus 1/*k* (s), the rate constant for each population (middle). (iii) Schematic showing the proposed time-dependent onset of different tiers of dynamics starting at time = 0 (the instant of photodissociation or the start of a measurement) that define the dynamic states of the protein (bottom). The B→A, C→A, and D→A transitions refer to the rebinding processes occurring within the B, C, and D states, respectively. The B→C and C→D designations indicate the dynamics-mediated transitions between states. The MEM distributions in this and subsequent figures show that there are multiple substates with distinct recombination rates within the B, C, and D states.

Temperature-Dependent Changes in the Kinetic Phases of R State [COHbA] Bathed in Glycerol. Figure 2 shows the temperature-dependent changes in the kinetic traces and associated MEM populations for the CO recombination in [COHbA]

(62) Samuni, U.; Juszczak, L.; Dantsker, D.; Khan, I.; Friedman, A. J.; Perez-Gonzalez-de-Apodaca, J.; Bruno, S.; Hui, H. L.; Colby, J. E.; Karasik, E.; Kwiatkowski, L. D.; Mozzarelli, A.; Noble, R.; Friedman, J. M. *Biochemistry* **2003**, *42*, 8272−8288.
(63) Gottfried, D.; Peterson, E.; Sheikh, A.; Yang, M.; Wang, J.; Friedman, J. *J. Phys. Chem.* **1996**, *100*, 12034−12042.
(64) Kumar, A. T. N.; Zhu, L.; Christian, J. F.; Demidov, A. A.; Champion, P. M. *J. Phys. Chem. B* **2001**, *105*, 7847−7856.
(65) Steinbach, P. J. *Biophys. J.* **1996**, *70*, 1521−1528.
(66) Steinbach, P. J.; Chu, K.; Frauenfelder, H.; Johnson, J. B.; Lamb, D. C.; Nienhaus, G. U.; Sauke, T. B.; Young, R. D. *Biophys. J.* **1992**, *61*, 235−245.
(67) Steinbach, P. J.; Ionescu, R.; Matthews, C. R. *Biophys. J.* **2002**, *82*, 2244−2255.
(68) Lavalette, D.; Tetreau, C.; Mouawad, L. *Biochem. Soc. Trans.* **2006**, *34* (Pt. 5), 975−978.

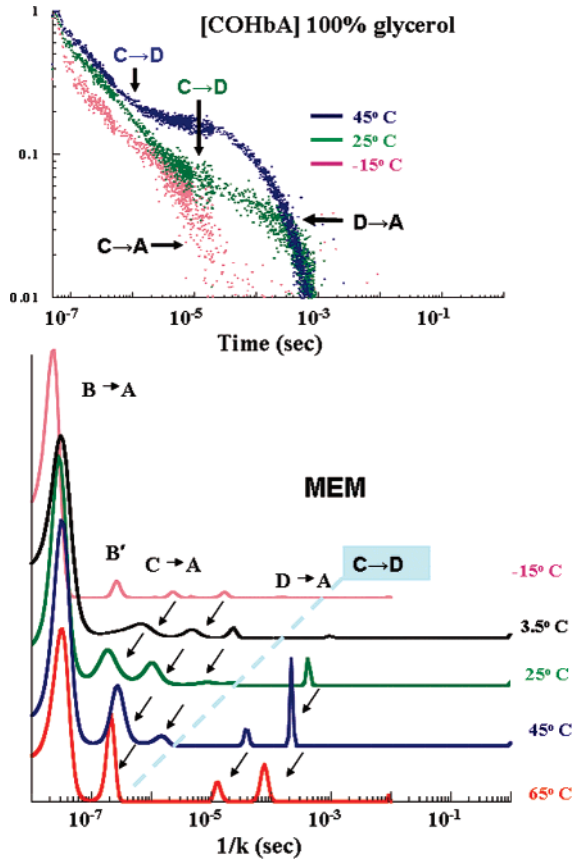

Figure 2. CO recombination traces and associated MEM distributions for a glycerol-bathed sample of sol−gel-encapsulated [COHbA] as a function of temperature. The light blue dashed line that cuts diagonally across the MEM populations shows the temperature-dependent change in the onset of the C→D transition. It can be seen that with earlier transition times there is a loss of those C→A phases that would occur to the right of the C→D dividing line. Additionally as the less distinct B→C transition gets faster, the B′→A phase is replaced by the fastest member of the C→A distribution. Thus, with increasing temperature there is an increasing fraction of the geminate recombination that is originating from the C state *vis-à-vis* the B state.

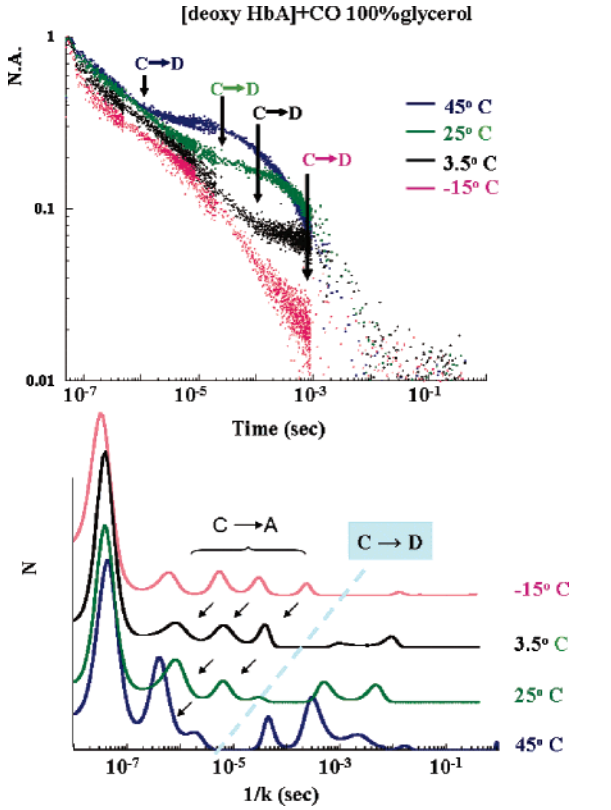

Figure 3. CO recombination traces and associated MEM distributions for a glycerol-bathed high-affinity T state sample (HT) of a [deoxyHbA]+CO as a function of temperature. (See Methods in the Supporting Information for a description.)

bathed in glycerol. At −15 °C, only the B→A and C→A kinetic phases are seen. As will be discussed in later sections, the C→D transition at this temperature under these conditions occurs at ∼1 ms, where for [COHbA] there is very little photoproduct population remaining. As the temperature is raised, the C→D transition occurs at progressively earlier time points, where eventually there is still an observable photoproduct population. As a consequence, one can now observe the appearance of the D→A recombination phase(s). It can also be seen both in the traces and in the MEM that the C→D transition eliminates those C→A phases that occur on a time scale the same as or slower than that of the transition. Thus, as the C→D transition occurs earlier (with respect to the dissociation event), one sees a progressive loss in the slower C state family of recombination phases (e.g., C″→A). Although not readily appreciated from this particular set of data, the increase in temperature also accelerates the onset of the B→C transition, such that the B′→A phase seen in the MEM for the −15 °C recombination is eliminated at the higher temperatures and is replaced by the thermally accelerated C→A phase. It can also be seen in the MEM that, with increasing temperature, there is a speeding up of many of the different kinetic phases but not the B→A phase, which appears to actually undergo a slight slowing on going from −15 to 3.5 °C. (A future publication will address the temperature dependence and activation energies of the individual MEM-based recombination processes.) The same progression seen with increasing temperature is also seen for sol−gel-encapsulated COHbA at a given temperature as a function of decreasing concentration of glycerol in the bathing buffer (see Supporting Information). The pattern seen in Figure 2 illustrates that the recombination trace for a given heme protein and ligand in a specific solvent at a given temperature is determined by the combination of B→C and C→D transition points and the nature of the recombination phases occurring within each of the three dynamic states.

Temperature-Dependent Changes in the Kinetic Phases of T State [deoxyHbA] +CO Bathed in Glycerol. Figure 3 shows the temperature dependence of the recombination traces and MEM populations for a [deoxyHbA]+CO sample that has evolved over a period of many days from the starting LT state conformation to an HT state population.[37] HT state refers to T state populations of liganded HbA that have undergone a ligand-binding-induced conformational evolution that includes a loosening the T state $\alpha_1\beta_2$ interface and a reduction in the proximal strain.[37,44,49,62] Functionally, the HT state relative to the LT state shows a higher geminate yield and faster bimolecular recombination but still not at the level of the R state.[37,44,62] The key feature in Figure 3 is that the same pattern as seen for the equilibrium distribution of liganded R state species (as seen in Figure 2) is seen for the T state species, but the C and D state kinetic phases are slower compared to the corresponding phase for the R state. The traces and the MEM show that the C→A and D→A phases for R and T start at the same time point in

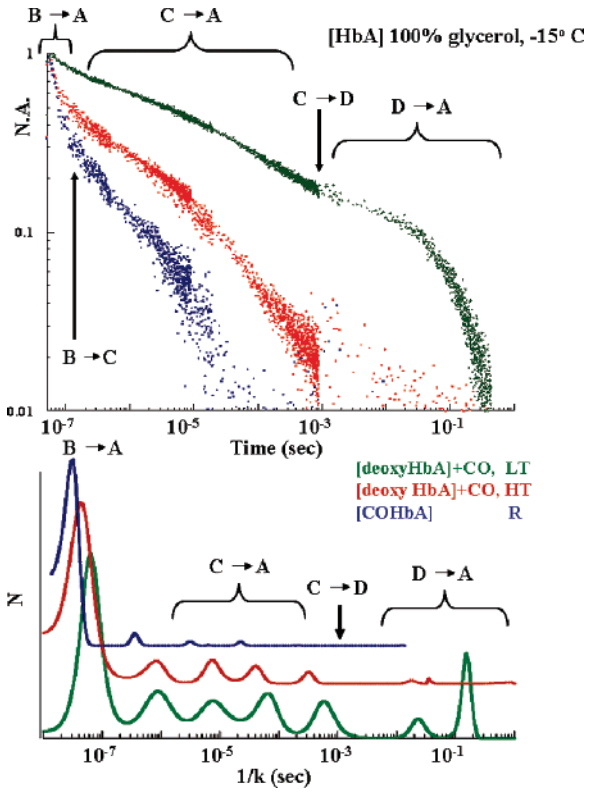

Figure 4. Comparison of the CO recombination traces and MEM populations at −15 °C for low-affinity T (LT, green), high-affinity T (HT, red), and R (blue) state [COHbA] samples encapsulated in a thin porous sol−gel matrix bathed in glycerol.

both cases, but for the T state samples there are additional subphases within C and D (see also Figure 1) that have the effect of slowing the overall composite phases. For example, at −15 °C, the overall C→A phase for [COHbA] is essentially over by 10 μs, whereas for the HT it extends another decade in time. The contribution of these several different C and D state subpopulations has the effect of making the trace for the composite C or D state recombination highly nonexponential. It can be seen how the extended T state C→A phase seen at −15 °C becomes progressively shortened with increasing temperature as the progressively earlier onset of the C→D transition successively terminates the C→A subphases, starting with the slowest and working its way toward the fastest phase. The progressive loss of the C→A phase with increasing temperature is not attributable to the temperature dependence of that phase. In a glassy matrix (not shown), where the α fluctuations are more strongly damped over this same temperature range, only minor temperature-dependent line shape changes are seen for the C→A recombination phase, as seen for Mb in a trehalose glass.[38,43] The changes seen in Figure 3 are fully consistent with a large temperature-dependent enhancement in the onset time for the C→D transition that progressively cuts into the time regime over which the C→A recombination would occur if D state dynamics were not activated.

T State Kinetic Traces as a Function of Tertiary State Conformation. Figure 4 compares the −15 °C kinetic traces and MEM populations from [COHbA] and two T state samples prepared as [deoxyHbA]+CO. The kinetic and spectroscopic properties of the sample in the green trace are indicative of the low-affinity T state distribution of conformations (designated as LT in the figure).[37,44] In contrast, the second such [deoxyHbA] +CO sample (red trace) displayed kinetic and spectroscopic properties of the high-affinity T state population (designated as HT in the figure). (See Methods section in the Supporting Information for details.)

In all three cases, the B→A and C→A phases dominate the overall kinetics, with only the LT sample showing a D→A phase. The MEM peaks are displayed with the amplitudes for the populations normalized with respect to the first B→A population. The MEM shows two clear-cut trends with respect to the B→A and C→A phases. The first trend evident from both the MEM and the kinetic traces is that, for the R state sample, a substantially larger fraction of the recombination occurs in the earlier phases compared to the T state samples. Similarly, a comparison of the traces and MEM for the LT and HT samples shows how the populations for the former are distributed among the slower phases to a much greater degree than for the latter sample (HT). In particular, it can be seen that, at the points of the B→C and C→D transitions, the geminate yield for both B and C state geminate phases follows the progression of R > HT > LT.

The second trend evident from the MEM populations shown in Figure 4 is that the B and C state recombination phases of the R state sample are faster than the corresponding phases of both T state samples. Most dramatic is the progression seen for the B→A MEM populations, with rates decreasing on going from R to HT to LT. The consequence is that, at the point of the B→C transition, more of the total recombination has occurred within the B state for R compared to HT compared to LT. At the time point of the C→D transition, there is no measurable remaining photoproduct for the R state left to undergo D→A recombination, whereas for the HT sample there is a trace of a D state recombination phase and for the LT sample there is a readily detectable D state population undergoing recombination. As noted earlier, the slowing of the different C state populations for both of the T state samples has the effect of stretching the overall C→A recombination over a longer time window due to the increased contribution from the slower C→A phases. In contrast, the R state sample has the C state population concentrated in the faster C substate populations, resulting in a kinetic trace for the overall C state recombination that is closer to being exponential, as would occur in the limit of just one MEM population for the C state. Indeed, for COHbA in a moderately dry trehalose-derived glassy matrix under these conditions (not shown), the MEM shows only a single C state population, and the C state recombination is even closer to having an exponential appearance, as reflected in a more vertical/less slanted slope.

In earlier studies in which the sol−gel samples were not bathed in pure glycerol, there is a progression of many kinetic traces as a [deoxyHbA]+CO sample evolved from the LT to the HT state.[37,44] The progression of traces and corresponding MEM distributions are consistent with a large number of intermediate states, but under the lower viscosity conditions employed in those studies, it was not completely clear whether these intermediate traces were the result of heterogeneous mixtures of LT, HT, and R states trapped in the sol−gel. The MEM populations shown in Figure 4 are not indicative of a mix of populations. Instead, they strongly support the conclusion that there are well-defined intermediates with a characteristic

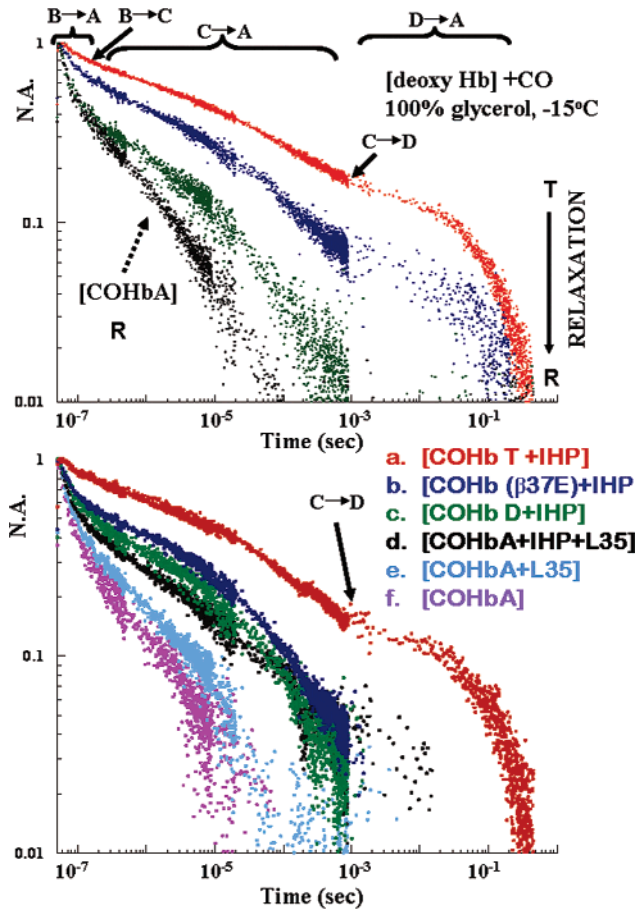

Figure 5. Comparison of CO recombination traces at −15 °C derived from glycerol-bathed sol−gel-encapsulated samples of both allosteric intermediates and stable endpoint species. The top series of traces shows the progression of kinetic patterns as an initial [deoxyHbA]+CO T state sample evolves toward the endpoint pattern associated with [COHbA]. The progression of traces from the [deoxyHbA]+CO samples are from samples that were allowed to evolve for progressively longer time periods (hours to weeks) prior to the addition of glycerol, which essentially stops the evolution. The bottom series of traces are derived from stable [COHb] samples, including both HbA and recombinant mutant Hb's in the presence and in the absence of allosteric effectors. (See the text for a description of the HbT, HbD, and Hb(Wβ37E) mutants.)

distribution of rates and amplitudes for the MEM populations associated with the intermediates. It appears that each intermediate has a characteristic set of kinetic rates reflected in the values for B, C, and D state MEM peaks associated with the intermediate. The resulting kinetic trace for the HT sample cannot be fit using a linear combination of R state and LT values (see Supporting Information).

The Multiple Kinetic Phases Seen for Transient Liganded T State Species Can Be Duplicated in Equilibrium Liganded Hb's. Figure 4 displayed two kinetic traces originating from [deoxyHbA]+CO samples that have evolved for different time periods subsequent to the addition of the CO. The top panel of Figure 5 shows more of the intermediate traces occurring during this progression. As in Figure 4, these traces are generated by adding the glycerol subsequent to a period of evolution subsequent to the addition of CO to the [deoxyHbA] sample. A more detailed account of these intermediates and their time evolution will be presented in a future paper. It appears that there is a clear progression with respect to the overall appearance of the traces as the sample evolves with time.

An obvious question is whether these kinetic patterns are derived from conformations that can be accessed under equilibrium conditions by suitable additions of effectors or mutagenic manipulations to HbA. The bottom panel of Figure 5 shows an arrangement of one such set of kinetic traces from a number of COHb's that indicates that the kinetic patterns derived from the LT→HT→R intermediates can be generated under equilibrium conditions. COHb T is a triple mutant of HbA (HbαL29F/αV96W/βN108K) that has been shown to remain in the T state when fully liganded in the presence of inositol hexaphosphate (IHP).[56,57] The liganded Hb(Wβ37E)+IHP remains stabilized in an HT conformation, as does the Hb D mutant (HbαV96W/βN108K, unpublished results). The most straightforward and consistent assessment of these findings is that the sol−gel does provide a means of trapping and tracking allosteric intermediates and that these intermediates can also be stabilized by mutagenic manipulation of HbA. The traces also show that the large range of kinetic patterns can be systematically analyzed from the perspective of the dynamic state model. The transition points for the dynamic state transitions are consistently at the same time points for a given set of solution/sol−gel conditions (see Supporting Information). The variations in the patterns observed under a given set of conditions are readily attributed to the different MEM-revealed kinetic populations within B, C, and D states. The results for the intermediates and modified forms of HbA show that there is systematic progression in these kinetic populations on going from low-affinity T to high-affinity T to R state. This plasticity in the tertiary state properties of HbA is consistent with the pattern of reactivity reported for HbA as a function of added allosteric effectors.[69−71]

Subunit Specificity in the Kinetic Patterns for T State Hb under High-Viscosity Conditions. Figure 6 shows the kinetic traces and MEM populations for three glycerol-bathed sol−gel-encapsulated T state samples: [deoxyHbA]+CO, [Hb(αCOFe/βZn)+L35/IHP], and [Hb(αZn/βCOFe)+L35/IHP] (where L35 is 2-[4-([3,5-dichlorophenyl)amino]carbonylamino)-phenoxy]-2-methylpropanoic acid). The kinetic trace and MEM populations are dramatically different for the two COFe/Zn hybrid Hb's. The [deoxyHbA]+CO sample appears to manifest a composite pattern. Whereas the β subunit displays a pattern that has noticeable contributions from the B, C, and D states, the α subunit, relative to the β subunit, shows an enhanced contribution from the B state, little or no C state contribution, and a slightly reduced D state contribution. Preliminary results on the temperature dependence of the kinetic pattern from the T state α subunit show a decrease in the B state contribution with increasing temperature, ultimately resulting in essentially a near-zero geminate yield, as seen in solution for this hybrid.[62] The pattern seen for the T state β subunit is very reminiscent of the pattern seen for wild-type Mb (horse and sperm whale),[26,27,43] where the C→A phase is attributed to geminate recombination under conditions where the dissociated ligand is accessing the Xe cavities and the recombination is being modulated by fluctuations and relaxations involving side chains of residues within the distal heme pocket, such as ValE11 and

(69) Tsuneshige, A.; Kanaori, K.; Samuni, U.; Danstker, D.; Friedman, J. M.; Neya, S.; Giangiacomo, L.; Yonetani, T. *J. Biol. Chem.* **2004**, *279*, 48959−48967.
(70) Tsuneshige, A.; Park, S.; Yonetani, T. *Biophys. Chem.* **2002**, *98*, 49−63.
(71) Yonetani, T.; Park, S. I.; Tsuneshige, A.; Imai, K.; Kanaori, K. *J. Biol. Chem.* **2002**, *277*, 34508−34520.

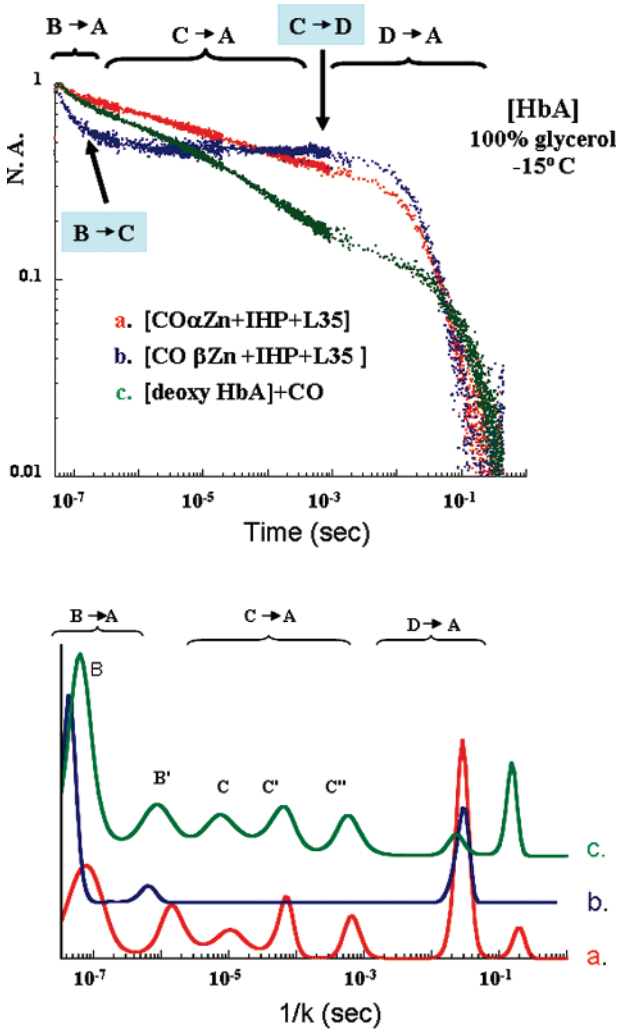

Figure 6. CO recombination traces and MEM populations at −15 °C for glycerol-bathed samples of encapsulated T state derivatives of HbA, including a fully liganded low-affinity T state derivative ([deoxyHbA]+CO) and half-liganded derivatives derived from the [α_2FeCO/β_2Zn] and [α_2Zn /β_2FeCO] iron−zinx symmetric hybrids of HbA. The half-liganded derivatives were encapsulated in the presence of a several-fold excess of IHP and L35 to ensure the stabilization of the low-affinity T state population.

HisE7. The absence of C state recombination phases for the T state α subunit may reflect fundamental differences between the two subunits with respect to accessible Xe cavities. The abrupt termination of the B→A phase in the kinetic trace from the T state α subunit kinetic is tentatively attributed to a fast, viscosity-dependent relaxation involving proximal heme−histidine interactions that increase proximal strain and thus substantially raise the barrier for recombination within the C state. Support for this relaxation-based hypothesis comes from preliminary time-resolved resonance Raman results that indicate the existence of a very fast and substantial viscosity-dependent relaxation involving the iron−proximal histidine stretching frequency. If indeed the absence of C state recombination phases of the T state α subunit has its origins at least in part due to enhanced proximal strain, then the rebinding within the D state of the T state α subunit likely occurs due to fluctuations of sufficient amplitude to increase the transient population of transition state heme configurations that have the iron in a more in-plane configuration. It has been argued that the transition state for the binding of CO to deoxy heme requires accessing a product-like transition state that has the iron in the heme plane configuration.[72,73]

Conclusions

The kinetic traces from both R and T state Hb's show the same trend observed in Mb's in that there is a temporal progression subsequent to photodissociation over which slower kinetic phases emerge. We have associated these emerging slower phases with dynamics-mediated processes that cause the slow-down in recombination rate. The presented results support both the concept of a solvent slaving-based hierarchy of dynamics that impact functional processes in a sequential fashion and the validity of using the new protein dynamic states model to dissect complex recombination traces from heme protiens. The sequential ordering of onset of dynamics-driven phenomena has a direct and compelling consequence for Hb (and Mb) reactivity, as reflected in the kinetic processes that contribute to such basic functionalities as ligand off rates, which help determine ligand delivery by heme proteins.

It appears that, for a given set of solution conditions, the transition point between kinetic phases is similar for both R and T state forms of Hb; however, each of the three observed kinetic phases is faster for the R state species. This pattern is consistent with an R−T-dependent barrier at the heme binding site, since that is the only obvious means of impacting kinetic phases originating both from highly localized sites within the distal heme pocket and from remote sites. A likely origin for this effect is that in the T state there is enhanced proximal strain and enhanced ValE11-derived steric effect in the α and the β subunits, respectively.[29,37,44,62,74,75] The kinetic patterns for the R and T state species show dramatic differences in terms of fractional composition of the different phases. This effect is readily explained in terms of competition between the conformation-dependent rates of the different kinetic phases for recombination and the solvent/temperature-dependent transition between protein dynamic states.

The systematic progression of kinetic traces having distinct MEM populations observed for both equilibrium and nonequilibrium samples is consistent with there being multiple functionally distinct intermediates associated with the transition from deoxy T to liganded R. Under high-viscosity conditions, the distinct MEM populations clearly show that these intermediates are not a simple two-state superposition of the initial T state and final R state populations. Furthermore, results are presented that show that these intermediates can be stabilized through mutagenic alterations of HbA as well as further manipulation through the addition of effectors. The array of recombination patterns associated with these different species fall into a systematic pattern that can be easily dissected using the dynamic state model. The results are consistent with the emerging models

(72) Friedman, J. M. *Methods Enzymol.* **1994**, *232*, 205−231.
(73) Ionascu, D.; Gruia, F.; Ye, X.; Yu, A.; Rosca, F.; Beck, C.; Demidov, A.; Olson, J. S.; Champion, P. M. *J. Am. Chem. Soc.* **2005**, *127*, 16921−16934.
(74) Unzai, S.; Eich, R.; Shibayama, N.; Olson, J. S.; Morimoto, H. *J. Biol. Chem.* **1998**, *273*, 23150−23159.
(75) Friedman, J. M.; Scott, T. W.; Fisanick, G. J.; Simon, S. R.; Findsen, E. W.; Ondrias, M. R.; Macdonald, V. W. *Science* **1985**, *229*, 187−190.
(76) Ackers, G. K.; Dalessio, P. M.; Lew, G. H.; Daugherty, M. A.; Holt, J. M. *Proc. Natl. Acad. Sci. U.S.A.* **2002**, *99*, 9777−9782.
(77) Ackers, G. K.; Holt, J. M.; Huang, Y.; Grinkova, Y.; Klinger, A. L.; Denisov, I. *Proteins* **2000**, Suppl. 4, 23−43.
(78) Scott, T. W.; Friedman, J. M. *J. Am. Chem. Soc.* **1984**, *106*, 5677−5687.

based on there being multiple functionally distinct tertiary/quaternary conformations contained within both the R and T state family of structures[44,76−80] that can be accessed under both equilibrium and nonequilibrium conditions.

(79) Viappiani, C.; Bettati, S.; Bruno, S.; Ronda, L.; Abbruzzetti, S.; Mozzarelli, A.; Eaton, W. A. *Proc. Natl. Acad. Sci. U.S.A.* **2004**, *101*, 14414−14419.
(80) Henry, E. R.; Bettati, S.; Hofrichter, J.; Eaton, W. A. *Biophys. Chem.* **2002**, *98*, 149−164.

Acknowledgment. This research was supported by National Institutes of Health Grants P01 HO071064 and RO1 AI52258.

Supporting Information Available: Details of the methods used in this work, including sol−gel encapsulation protocols, trehalose matrix encapsulation, kinetics setup, and the maximum entropy method. This material is available free of charge via the Internet at http://pubs.acs.org.

JA072342B